# Preparation of Highly Exfoliated and Transparent Polycarbonate/Clay Nanocomposites by Melt Blending of Polycarbonate and Poly(methyl methacrylate)/Clay Nanocomposites

**Saptarshi Dhibar, Prativa Kar, B. B. Khatua**

*Materials Science Centre, Indian Institute of Technology, Kharagpur 721302, India*

Received 27 September 2011; accepted 20 December 2011
DOI 10.1002/app.36678
Published online 2 February 2012 in Wiley Online Library (wileyonlinelibrary.com).

**ABSTRACT:** In this report, we introduce an industrially feasible method that involves melt blending of polycarbonate (PC) and *in situ* suspension polymerized exfoliated PMMA/clay ($Na^+$MMT) nanocomposites to prepare highly exfoliated PC/clay nanocomposites. The rational behind this is that PC is well known to form miscible blend with low molecular weight PMMA. Thus, low molecular weight PMMA/clay exfoliated nanocomposites were prepared by suspension polymerization using pre-exfoliated clay ($Na^+$MMT) in water media during the polymerization. The (80/20 w/w) PC/PMMA blends without and with $Na^+$MMT showed single glass transition temperature ($T_g$), indicating complete miscibility of the polymers in the blend. The surface morphologies of the composites were studied by scanning electron microscopy (SEM). Wide-angle X-ray diffraction and transmission electron microscope (TEM) studies of the nanocomposites revealed delamination of the clay silicate layers in the PC matrix. The properties of the (80/20 w/w) PC/PMMA-$Na^+$MMT nanocomposites were significantly higher than that of the pure PC. Moreover, retention of the optical transparency of PC in the nanocomposites could be due to the presence of unmodified clay ($Na^+$MMT), which did not contain any organic modifier (quaternary ammonium salt) that could decompose during melt mixing of PC at high temperature ($\approx 280^\circ C$). © 2012 Wiley Periodicals, Inc. J Appl Polym Sci 125: E601–E609, 2012

**Key words:** PC; clay; dispersions; nanocomposites; exfoliation

## INTRODUCTION

Polymer-layered silicate nanocomposites (PLSNs) have received much interest over the past decade as an alternative to conventional filled composites because of their unexpected properties, and the potential of becoming a new class of high-performance engineering materials.[1,2] As a rule, homogeneous dispersion of $3 \sim 5$ wt % of thin clay layers improves the mechanical and thermal properties of the polymer matrix to the same extent as 30–50 wt % of micron-sized fillers.[3–5] However, homogeneous dispersion of hydrophilic clay silicates in polymer matrix requires proper modification of the inorganic clay in order to improve the polymer-clay compatibility.

Polycarbonate (PC) has outstanding impact strength and good optical clarity and is used widely in many transparent engineering applications. The drawbacks of PC are its poor chemical resistance and low resistance to abrasion. Thus, PC has been modified and tailored in many different ways, particularly by blending with other polymers for use in demanding applications.[6] Recently, the nanocomposites technology has also been applied in the modification of PC, compounding with clay mineral to improve the physical and chemical properties of PC materials. Many works have been reported on the preparation and characterization of PC/clay nanocomposites.[7–17] The nanoscaled morphology, mechanical properties, thermal stability, and color formation as well as crystallization behavior of PC/clay nanocomposites are investigated extensively.

Gonzalez et al.[7] prepared PC/clay nanocomposites by melt-mixing PC with polycaprolactone (PCL)/organoclay masterbatch. The nanocomposites revealed a mixed intercalated/exfoliated clay morphology and 55% increase in modulus of PC in the presence of 5 wt % clay in the nanocomposites. Carrion et al.[8] reported the intercalation of clays in melt-extruded PC/organoclay nanocomposites. A reduction in $T_g$ of the PC in the nanocomposites was explained in terms of plasticizing effect of the clay. Paul et al.[9] studied the effect of molecular weight of PC and modifier (alkyl amine) structure on the morphology of melt-extruded PC/clay nanocomposites with various amine-modified clays. They reported that miscibility of the modifier with PC led to the

*Correspondence to:* B. B. Khatua (khatuabb@matsc.iitkgp.ernet.in).

formation of partially exfoliated clay morphology in the nanocomposites. Paul et al.[10] also reported that the color formation in melt extruded PC/clay nanocomposites depend on the structure of the organoclay, and the presence of double bond in the hydrocarbon tail of the surfactants led to more darkly colored materials than the saturated surfactants. Mitsunaga et al.[11] reported the formation of intercalated PC/clay nanocomposites through melt extrusion method in the presence of a compatibilizer. Lee et al.[12] reported exfoliation of PC/organoclay (Cloisite 30B) nanocomposites prepared by melt blending in a twin-screw extruder and proposed that the driving force behind exfoliation was originated from hydrogen bonding. Smith et al.[13] showed that the color formation during melt blending of PC with a copolyester caused by the interaction of residual titanium catalyst in the copolyester with the phenolic end groups of the PC. Yoo et al.[14] reported that microwave-aided solid-state polymerization is the more effective way to achieve exfoliation in PC/clay nanocomposites rather than the conventional solid-state polymerization using oil heating. Swaminathan et al.[15] prepared the PC/clay nanocomposites via *in situ* melt polycondensation using phosphonium- and imidazolium-modified nanoclays without and with reactive functionality (bisphenol-A). The modifier containing reactive bisphenol-A group resulted in the formation of exfoliated PC/clay nanocomposites whereas intercalated or phase separated structures were obtained in absence of reactive functionality in the modifier chain. Brittain et al.[16] reported the synthesis of intercalated and partially exfoliated PC/clay nanocomposites from PC cyclic oligomers and an organically modified layered silicate. Nevalainen et al.[17] showed the effect of two commercial surface-modified montmorillonite organoclays on the morphology and properties of PC nanocomposites and determined the extent to which organoclays could be dispersed in a PC matrix by melt processing.

Till date, considerable amount of research work has been devoted to prepare PC/clay nanocomposites through various conventional methods. However, in most of the cases, not only the intercalated clay morphology but also the development of the color in the nanocomposites limited the application of PC/clay nanocomposites. PC is susceptible to a variety of chemical processes caused by thermal and oxidative degradation mechanism at elevated temperature during melt processing[18–21]; these reactions may be significantly aggravated in presence of nanofillers. A specific concern is that the quaternary ammonium alkyl surfactants in the organoclay undergo complex degradation reaction at high temperature ($\geq$180°C).[13,14,22] In addition, a variety of metals ions exist in natural clays,[23,24] and the degradation products of these constituents may trigger various reactions and color formation process in PC. In this article, we introduced industrially feasible method that involves melt blending of PC and *in situ* suspension polymerized exfoliated PMMA/clay ($Na^+$MMT unmodified clay) nanocomposites to prepare the PC/clay nanocomposites. The rational behind this is that PC is well known to form miscible blend with low molecular weight PMMA.[25–31] Thus, low molecular weight PMMA clay nanocomposites were prepared by suspension polymerization using pre-exfoliated clay ($Na^+$MMT) in water media during the polymerization. We found that in (80/20 w/w) PC/PMMA-$Na^+$MMT blend the final properties of the nanocomposites were significantly higher than that of the pure PC. Here, we discuss the detail of our findings.

## EXPERIMENTAL

### Materials used

Methyl methacrylate (MMA) monomer used in this study was of synthetic grade and was procured from Merck, Germany. Benzoyl peroxide (BP) and poly(vinyl alcohol) (PVA) were supplied by Loba Chemie, Mumbai, India. The unmodified clay (sodium montmorillonite, $Na^+$MMT) used in this study was supplied by Southern Clay Products. The cation exchange capacity (CEC) of $Na^+$MMT is 92.6 mequiv/100 g of clay. The $Na^+$MMT was used without any further purification, and hereafter, $Na^+$MMT is referred to as the clay. The bisphenol-A PC used in this study was of commercial grade (Lexan 143, MFI $\approx$ 10.5 g/10 min at 300°C and 1.2 Kg load) procured from SABIC Innovative Plastics.

### Synthesis of PMMA/$Na^+$MMT nanocomposites by *in situ* suspension polymerization

In a 500-mL separating funnel, 100 mL of MMA monomer was taken and 20 mL of 5 wt % NaOH solution was added. After shaking the mixture for 15 min, the purified MMA was decanted into a 250-mL beaker. This process was repeated for five times. Finally, the purified MMA was collected after washing with deionized water.

Desired amount (1.5 g) of PVA was taken in a three-neck reactor containing 1 L of deionized water. The mixture was stirred for 1 h at 85°C. In another beaker, 0.5 g of $Na^+$MMT clay was dispersed in 300 mL of deionized water and ultrasonicated for 1 h to exfoliate the clay platelets in the water. The sonicated water/$Na^+$MMT mixture was added into the PVA solution under continuous stirring. Purified MMA (50 mL) and BP (0.5 g) were taken in a 250-mL beaker, and the mixture was stirred for 1 h by using a magnetic stirrer at room temperature. Finally, the mixture of MMA and BP was slowly added into the

reactor. The reaction was carried out under a nitrogen ($N_2$) atmosphere, first at 80°C for 4 h and then at 90°C for 1 h. The resulting dispersion was filtered and the PMMA-$Na^+$MMT particles were rinsed with water and methanol several times and dried under vacuum at 80°C overnight. From the final weight (≈ 35 g) of the PMMA-$Na^+$MMT nanocomposites, the loading of clay in the nanocomposites was calculated to be ≈ 1.45 phr (parts per hundred resin). Pure PMMA was also synthesized by following the same polymerization procedure.

The viscosity average molecular weight of the suspension polymerized PMMA and tetrahydrofuran (THF) extracted PMMA in PMMA-clay nanocomposites was determined by viscometric method in chloroform, following the Mark-Houwink equation[32]:

$$\eta = KM_v^a,$$

where $\eta$ is the viscosity of the solution, $K = 0.34 \times 10^{-4}$ and $a = 0.83$ at 25°C for chloroform.

The calculated viscosity-average molecular weight of the pure PMMA and the PMMA extracted from the composites were found to be ≈ 25,460 and ≈ 22,618, respectively. The presence of clay may affect the polymerization kinetics and mechanisms that reduce the polymer molecular weight and change its molecular-weight distribution.[33]

### Preparation of PC/PMMA-$Na^+$MMT nanocomposites

PC/PMMA blend (80/20 w/w) and PC/PMMA-$Na^+$MMT nanocomposites was prepared by melt blending of PC with PMMA or, PMMA-$Na^+$MMT nanocomposites in an internal mixer (Brabender Plasticorder, S. C. Day, Kolkata, India) at 280°C. The mixing was carried out at 40 rpm for 15 min. To avoid moisture-induced thermal degradation, all the polymer and the clay were completely dried in a vacuum oven at 80°C for 36 h before melt blending. The melt mixed PC/PMMA-clay nanocomposites was cooled at room temperature and finally injection molded at the same temperature under constant pressure. The loading of clay in the (80/20 w/w) PC/PMMA-$Na^+$MMT nanocomposites was calculated to be 0.287 phr.

## CHARACTERIZATION

### Surface morphology study

A scanning electron microscope (SEM, VEGA II LSU, TESCAN, Czech Republic) was used to study the surface morphology of the PC/PMMA and PC/PMMA-$Na^+$MMT nanocomposites. The injection molded samples were broken inside the liquid nitrogen. The fractured surface of the samples was coated with a thin layer of gold to avoid electrical charging, and SEM images were taken on the fracture surface, at an operating voltage of 10 kV.

### Differential scanning calorimetry study

The glass transition temperature ($T_g$) of the pure PC, PMMA, and the PC/PMMA-clay nanocomposites was determined by differential scanning calorimetry (DSC; DSC-200 PC, NETZSCH) under $N_2$ atmosphere. The second heating curves of the pure PC, PMMA, and PC/PMMA-clay nanocomposites were taken for the determination of the $T_g$. The heating and cooling rate was 10°C/min.

### Wide-angle X-ray diffraction study

The *d*-spacing (gallery height) of the clay itself as well as that in the nanocomposites was examined by using wide-angle X-ray diffractometer (Rigaku XRD, Ultima-III, Japan) with nickel-filtered Cu K$\alpha$ line ($\lambda = 0.15404$ nm) operated at 40 kV and 100 mA and scanning rate of 0.5°/min. The sample-to-detector distance was 400 mm. The gallery height was calculated by Bragg's law $d = n\lambda/2 \sin\theta$, where, *d* is the *d*-spacing, $\lambda$ is the wave length of the incident wave, and $\theta$ is the angle between the incident ray and the scattering planes and *n* is an integer.

### TEM analysis

The extent of dispersion of the clay silicates in the PC/PMMA-clay nanocomposites was studied by transmission electron microscopy (HRTEM: JEM-2100, JEOL, Japan), operating at an accelerating voltage of 200 kV. The nanocomposites sample was ultra-microtomed at cryogenic condition with a thickness of 60 ~ 80 nm. As the clay has much higher electron density than neat polymers, it appeared dark in TEM images.

### Thermal analysis

The thermal stability (the onset degradation temperature and the temperature corresponding to 50% weight loss and maximum weight loss) of the pure PC, PMMA, and the nanocomposites were investigated using a thermogravimetric analyzer (TGA-209F, from NETZSCH, Germany). The sample was heated from room temperature to 600°C at a heating rate of 10°C/min under air atmosphere.

### Dynamic mechanical analysis

Thermomechanical properties (storage modulus) of the pure polymers, blend and nanocomposites were measured with the injection molded sample by using a Dynamic Mechanical Analyzer (DMA 2980

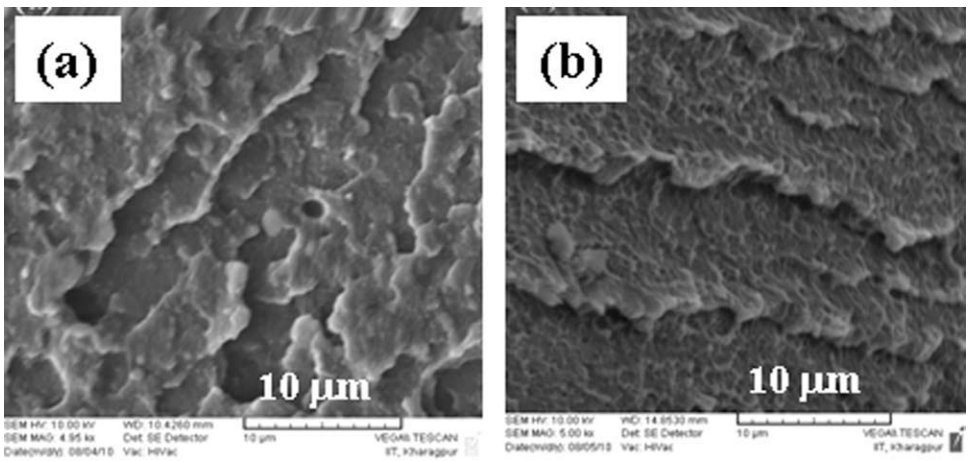


**Figure 1** SEM images of (a) (80/20 w/w) PC/PMMA blend; and (b) (80/20 w/w) PC/PMMA-$Na^+$MMT nanocomposites with 0.287 phr clay.

model, TA Instruments, USA), in tension film mode at a constant vibration frequency of 1 Hz, temperature range of 30–150°C at a heating rate of 5°C/min in nitrogen atmosphere. The dimension of the specimen was 30 × 6.40 × 0.45 $mm^3$.

### UV–vis spectroscopy

To obtain the thermal degradation and the color formation of the PC nanocomposites, UV–vis spectra were carried out using the solution spectra techniques. At first pure PC, pure PC/PMMA blend, PMMA/$Na^+$MMT, and the PC/PMMA-$Na^+$MMT nanocomposites were dissolved in dichloromethane solution (DCM). The percent (%) of transmittance was measured by using Perkin Elmer, Lambda 750 spectrophotometer.

## RESULTS AND DISCUSSION

Many researchers have reported on the preparation and characterization of PC/clay nanocomposites by using organoclays.[7–17] However, irrespective of the method of composites preparation, the possible use of PC/clay nanocomposites has been limited not only by the intercalated clay morphology in the nanocomposites[11,15,16] but also the challenges to retain optical transparency of PC in the nanocomposites.[10,13] Most of the studies on PC/clay nanocomposites used quaternary ammonium containing modifiers, which, at the processing temperature (~ 280°C) of the PC, decompose via the Hoffman elimination reaction resulting in the formation of *t*-amines. Amines are known to induce base catalyzed chain scission of PC leading to molecular weight reduction and color formation in the final nanocomposites.

PC and PMMA are two important transparent polymers widely used in many optical applications. However, some inferior properties of these two polymers often limit their applications. PMMA exhibits excellent transparency and high-surface hardness with low-impact strength and low-heat resistance. In contrast, PC has superior toughness and a very high glass transition temperature, but its surface hardness is low. Blends of PC and PMMA have received considerable attention[34–38] because of their potential applications as gas separation membrane, substrate of the optical data storage discs, packaging materials. In general PC/PMMA blends are prepared by melt extrusion or solution casting techniques with or without compatibilizers. Among a number of PMMA blends studied for miscibility, PC with PMMA is one of the most thoroughly investigated blends, due to excellent properties of the PC, including outstanding ductility, low water absorption, and high glass transition temperature ($T_g$). PC is reported to form miscible blends with low molecular weight ($M_w$: 14,800 ~ 44,000) PMMA.[25–31]

### Surface morphology study by SEM

Phase morphology of the (80/20 w/w) PC/PMMA blends, without and with unmodified nanoclay ($Na^+$MMT), is shown in Figure 1. The SEM image of the (80/20 w/w) PC/PMMA blend shown in Figure 1(a), clearly demonstrated a one-phase structure, indicating the miscibility of the blend components, and it was not possible to distinguish any dispersed domain at this magnification. The difference in contrast in the image was due to the roughness of the cryofractured surface. Figure 1(b) represents the SEM image of the melt-mixed (80/20 w/w) PC/PMMA-$Na^+$MMT nanocomposites containing 0.287 phr clay. As observed, the micrograph revealed similar extent of miscibility of the component polymers in the blend/clay nanocomposites, as was in case of (80/20 w/w) PC/PMMA blend.

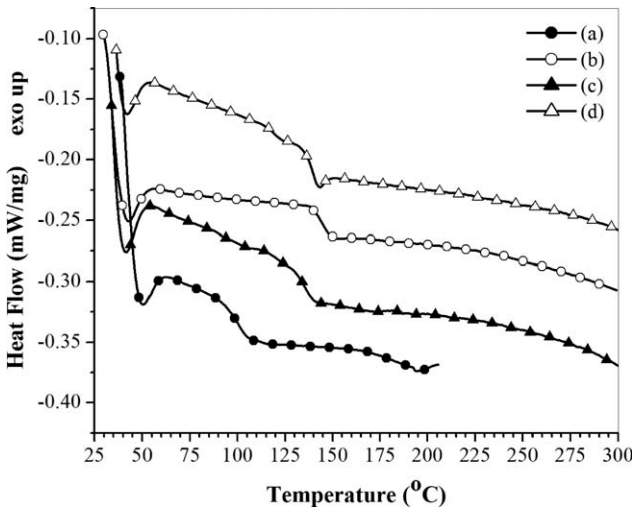


**Figure 2** DSC thermograms of (a) pure PMMA; (b) pure PC; (c) (80/20 w/w) PC/PMMA blend; and (d) (80/20 w/w) PC/PMMA-$Na^+$MMT nanocomposites with 0.287 phr clay.

## DSC study

The effect of the dispersion of the clay platelets on the glass transition temperature ($T_g$) was studied using DSC. Figure 2 shows the DSC scans of the *in situ* polymerized PMMA, pure PC, (80/20 w/w) PC/PMMA blend and PC/PMMA-$Na^+$MMT nanocomposites. From the DSC scan, it can be observed that the $T_g$s of the pure PMMA and PC were 103 and 145°C, respectively. In case of the (80/20 w/w) PC/PMMA blend, a single $T_g$ was observed at 136°C, which revealed the formation of single phase in the blend, in agreement with the SEM results. Again (80/20 w/w) PC/PMMA-$Na^+$MMT nanocomposites containing 0.287 phr clay showed only one distinct $T_g$ at 141°C, which implied single phase behavior of the blend in presence of $Na^+$MMT clay. The $T_g$ of the (80/20 w/w) PC/PMMA-$Na^+$MMT nanocomposites was slightly higher than the (80/20 w/w) PC/PMMA blend. For instance, the $T_g$ of PC/PMMA blend (136°C) was increased to 141°C in the PC/PMMA-$Na^+$MMT nanocomposites. The increase in $T_g$ of the (80/20 w/w) PC/PMMA blend in presence of clay was due to the intercalation of PC and PMMA chains into the clay galleries, which restricted the segmental motions of the polymer chains.

## X-ray diffraction study

Figure 3 shows the wide-angle X-ray diffraction (WAXD) patterns of the pure PC, PMMA, PMMA-$Na^+$MMT (1.45 phr) nanocomposites, (80/20 w/w) PC/PMMA blend and its nanocomposites with 0.287 phr clay. The WAXD pattern of pure $Na^+$MMT [Fig. 3(a)] showed a characteristic peak at $2\theta \approx 6.90°$ corresponding to the gallery height ($d_{001}$ spacing) of 1.28 nm. The characteristic peak of the clay did not appear in the *in situ* suspension polymerized PMMA-$Na^+$MMT (1.45 phr) nanocomposites [Fig. 3(b)]. This indicated the extensive layer separation associated with the high level of delamination of the clay silicate layers in the PMMA matrix, resulting in the high level of exfoliation of the clays. The WAXD pattern of (80/20 w/w) PC/PMMA-$Na^+$MMT nanocomposites [Fig. 3(d)] also indicated the absence of any characteristic peak of the clay, suggesting the presence of highly exfoliated clay silicate layers in the nanocomposites. We conclude that exfoliated clay platelets presented in the suspension polymerized PMMA-$Na^+$MMT nanocomposites were homogeneously dispersed throughout the PC/PMMA matrix without any stacking of silicates after melt mixing of PMMA-$Na^+$MMT nanocomposites and PC.

## TEM analysis

The extent of dispersion of the clay silicates in the *in situ* polymerized PMMA-$Na^+$MMT nanocomposites and PC/PMMA-$Na^+$MMT nanocomposites was investigated by TEM analysis, as shown in Figure 4. The dark lines in the images correspond to the intersections of the silicate layers, and the bright areas denote the composites matrix (polymer). As observed, in PMMA-$Na^+$MMT (1.45 phr) nanocomposites [Fig. 4(a)], the majority of the clay platelets were homogeneously dispersed with delaminated clay morphology (marked with arrows) and minor amount (marked with circles) of clays were in close proximity to exfoliation in the PMMA matrix. This could be due to high loading (1.45 phr) of the clay

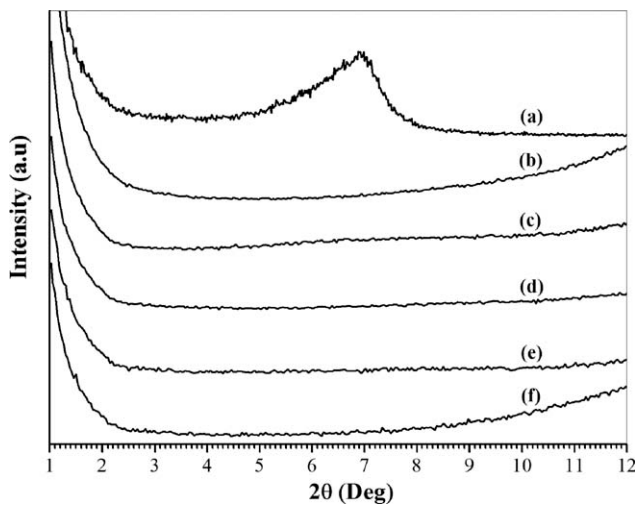


**Figure 3** XRD pattern of (a) pure $Na^+$MMT; (b) PMMA-$Na^+$MMT (1.45 phr); (c) (80/20 w/w) PC/PMMA blend; (d) (80/20 w/w) PC/PMMA-$Na^+$MMT nanocomposites with 0.287 phr clay; (e) pure PC; and (f) pure PMMA.

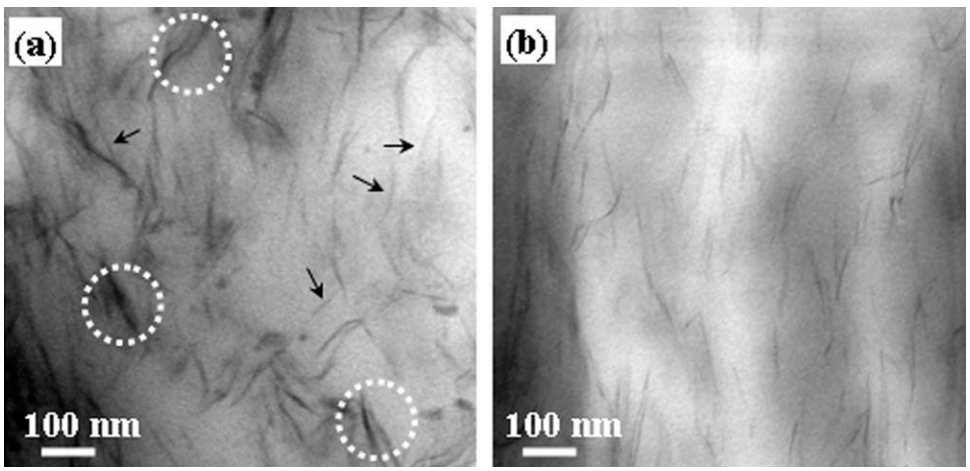


**Figure 4** TEM image of (a) PMMA-$Na^+$MMT (1.45 phr) nanocomposites; and (b) (80/20 w/w) PC/PMMA-$Na^+$MMT nanocomposites containing 0.287 phr clay.

in the PMMA matrix. Interestingly, the TEM image [Fig. 4(b)] of (80/20 w/w) PC/PMMA-$Na^+$MMT nanocomposites did not exhibit any stacking structure of the clay silicates in the PC/PMMA matrix. The clay layers lost their stacking structure and disorderly dispersed in the PC/PMMA matrix. We assumed that the applied shear force during melt-mixing of PC and PMMA-$Na^+$MMT led to homogeneous dispersion and individualization of the near exfoliated clay platelets presented in the PMMA-$Na^+$MMT (1.45 phr) nanocomposites and thus, exfoliation of the clays in the miscible PC/PMMA blend matrix. Based on the TEM micrographs, it can be concluded that high exfoliation of the clay was achieved in the (80/20 w/w) PC/PMMA-$Na^+$MMT nanocomposites with 0.287 phr clay loading.

## Dynamic mechanical analysis

The viscoelastic properties of the pure PC, PMMA, and their nanocomposites were measured as a function of temperature by dynamic mechanical analysis (DMA). The storage modulus of the pure PC, pure PMMA, (80/20 w/w) PC/PMMA blend and (80/20 w/w) PC/PMMA-$Na^+$MMT nanocomposites are shown in Figure 5. It was observed that in both glassy and rubbery regions, the storage modulus of the virgin blend and the PC/PMMA-$Na^+$MMT nanocomposites were higher than that of the neat PC. At 40°C, the storage modulus (1.70 GPa) of the neat PC was increased to 2.02 GPa and 2.06 GPa for the virgin PC/PMMA blend and the blend-clay nanocomposites, respectively. At high temperature region (above $T_g$), the storage modulus of the (80/20 w/w) PC/PMMA-$Na^+$MMT nanocomposites was also higher than the (80/20 w/w) PC/PMMA blend but lower than the neat PC. This increase in storage modulus of nanocomposites compared with blend indicates the reinforcing effect imparted by the high aspect ratio clay platelets that allowed a greater degree of stress transfer at the interface. Furthermore, restricted segmental motion at the organic–inorganic interface due to confinement of the polymeric chains inside the clay galleries at the nanoscale level may be the possible cause for increase in the storage modulus.

The loss modulus of the pure PC, pure PMMA, (80/20 w/w) PC/PMMA blend, and its nanocomposites are shown in Figure 6. It was observed that the loss modulus of PMMA was increased from 236 MPa to 258 MPa in (80/20 w/w) PC/PMMA blend and to 273 MPa in the (80/20 w/w) PC/PMMA-$Na^+$MMT nanocomposites with 0.287 phr clay. The variation of tan δ as a function of temperature is

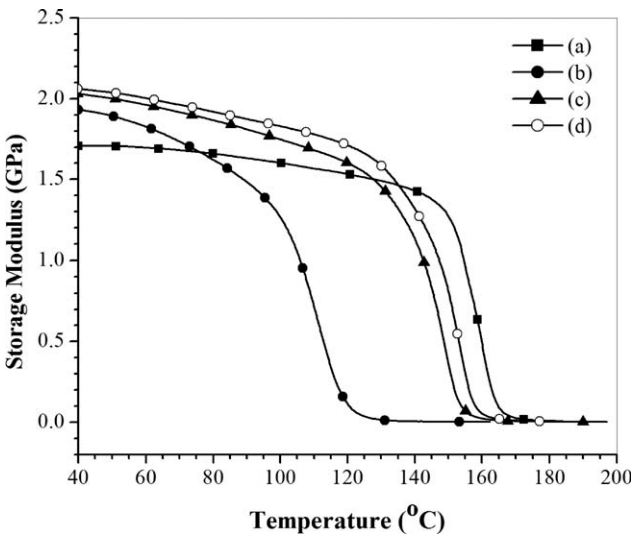


**Figure 5** Plot of storage modulus vs. temperature of (a) pure PC; (b) pure PMMA; (c) (80/20 w/w) PC/PMMA blend; and (d) (80/20 w/w) PC/PMMA/$Na^+$MMT nanocomposites with 0.287 phr clay.

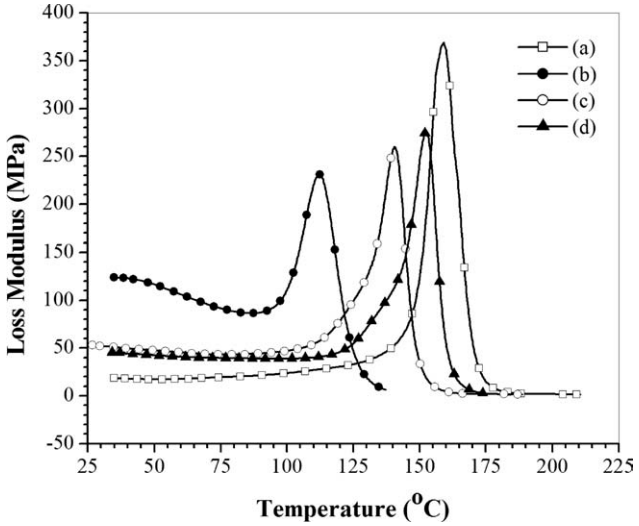


**Figure 6** Plot of loss modulus vs. temperature of (a) pure PC; (b) pure PMMA; (c) (80/20 w/w) PC/PMMA blend; and (d) (80/20 w/w) PC/PMMA/$Na^+$MMT nanocomposites with 0.287 phr clay.

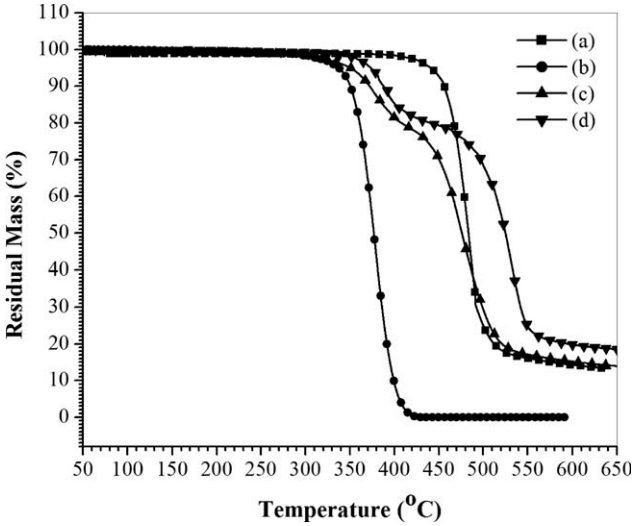


**Figure 8** TGA thermogram of (a) pure PC; (b) pure PMMA; (c) (80/20 w/w) PC/PMMA blend; and (d) (80/20 w/w) PC/PMMA-$Na^+$MMT nanocomposites with 0.287 phr clay.

shown in Figure 7. It was observed that the tan δ curve of pure PMMA showed a peak at ≈ 127°C, correspond to the glass transition temperature of PMMA. Pure PC showed a tan δ peak at ≈ 158°C, which correspond to its glass transition temperature. Generally, for an immiscible blend, the tan δ versus temperature curve shows the presence of two tan δ or damping peaks corresponding to the glass transition temperatures of the component polymers.[39–42] For a highly compatible blend, the curve shows only a single peak between the transition temperatures of the component polymers,[39] whereas broadening of the transition peak occurs in the case of partially compatible system.[42] In the case of compatible and partially compatible blends, the glass transition temperatures shifted to higher or lower temperatures as a function of the compositions. The (80/20 w/w) PC/PMMA blend showed single tan δ peak at ≈ 155°C and the (80/20 w/w) PC/PMMA-$Na^+$MMT nanocomposites showed single tan δ peak at ≈ 159°C. These results led us to conclude that PC/PMMA formed a miscible blend in absence and presence of the $Na^+$MMT clay.

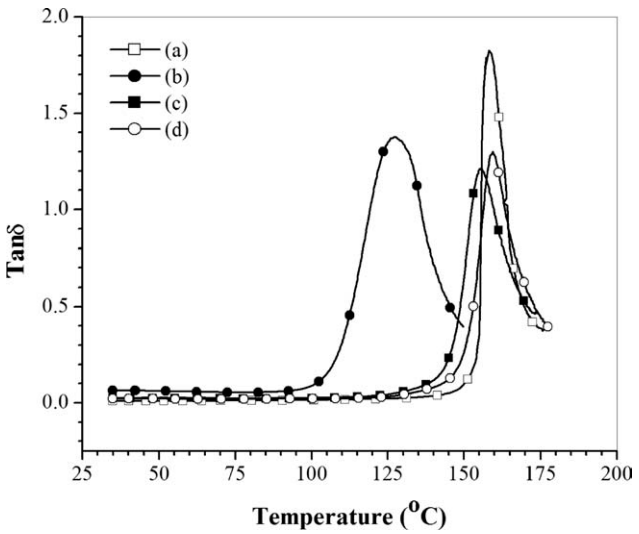


**Figure 7** Plot of tan δ versus temperature of (a) pure PC; (b) pure PMMA; (c) (80/20 w/w) PC/PMMA blend; and (d) (80/20 w/w) PC/PMMA/$Na^+$MMT nanocomposites with 0.287 phr clay.

### Thermogravimetric analysis

The thermal stability of the pure PC, pure PMMA, and its nanocomposites with unmodified clay has been studied by thermogravimetric analysis (Fig. 8). From the TGA curve, the onset degradation temperature ($T_1$), temperature corresponds to 50% weight loss ($T_{50}$), and maximum weight loss ($T_{max}$) were calculated and shown in Table I. It is reported that the incorporation of clay platelets into the polymeric materials improves the thermal stability of the polymer–clay composites depending on the degree of dispersion of the clay silicates in the matrix polymer.[2,11,43–48] It was observed that the onset degradation temperature ($T_1$ ≈ 314°C) of the pure PMMA was increased significantly in the (80/20 w/w) PC/PMMA blend ($T_1$ ≈ 325°C) and (80/20 w/w) PC/PMMA-$Na^+$MMT nanocomposites ($T_1$ ≈ 354°C). From the curves, it was seen that (80/20 w/w) PC/PMMA blend and PC/PMMA-$Na^+$MMT nanocomposites showed two degradation peaks; the first one was for PMMA and the second one was for the PC. It was also observed that the $T_1$ for the blend and nanocomposites were appeared in between the $T_1$ of

**TABLE I**
**TGA Results of Pure Polymers and Their (80/20 w/w) Blend-Clay Nanocomposites**

| Sample | $T_1$ (°C) | $T_{50}$ (°C) | $T_{max}$ (°C) | % Wt. loss (max) |
|---|---|---|---|---|
| PMMA | 314 | 377 | 443 | 99.73 |
| PC | 427 | 482 | 564 | 84.55 |
| (80/20 w/w) PC/PMMA blend | 325 | 476 | 566 | 84.00 |
| (80/20 w/w) PC/PMMA-$Na^+$MMT nanocomposites with 0.287 phr clay | 354 | 527 | 603 | 80.33 |

the pure PMMA and PC. The temperature corresponding to 50% weight loss of the pure PC ($T_{50} \approx$ 482°C) was also increased in the (80/20 w/w) PC/PMMA-$Na^+$MMT nanocomposites ($T_{50} \approx$ 527°C) containing 0.287 phr clay. The exfoliated clay silicate layers acted as a superior insulator and mass transport barrier to the products generated during decomposition which enhanced the thermal stability.

## UV–vis spectroscopy

The optical clarity of the pure PC, (80/20 w/w) PC/PMMA blend, and exfoliated PC/PMMA-$Na^+$MMT nanocomposites was measured by UV–vis spectrophotometer. Figure 9 shows the UV–vis spectra of pure PC, PC/PMMA blend, PC/PMMA-$Na^+$MMT nanocomposites with 0.287 phr clay. During the monitoring of the entire visible-light wavelength (400–700 nm), the optical transmission of 99.45% of the wavelength at 700 nm was obtained for the pure PC. The PC/PMMA-clay nanocomposites showed a slight decline in transmission in the visible light region and it can be seen from the Figure 9(c) that the nanocomposites still retain a high optical transmission of $\sim$ 98%. The retention of high optical transparency of PC in the nanocomposites could be due to the presence of unmodified clay ($Na^+$ MMT), which did not contain any organic modifier (quaternary ammonium salt) that could decompose during melt mixing of PC at high temperature ($\approx$ 280°C).

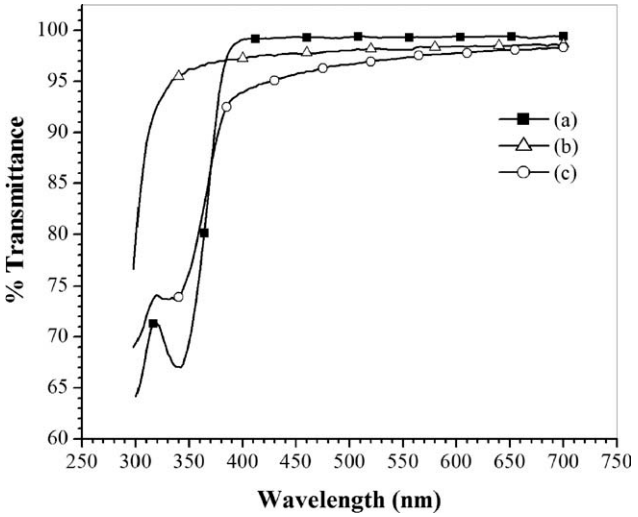


**Figure 9** Plot of light transmittance of (a) pure PC; (b) (80/20 w/w) PC/PMMA blend; and (80/20 w/w) PC/PMMA-$Na^+$MMT nanocomposites with 0.287 phr clay.

The optical transparency of the pure PC and its nanocomposites has also been verified through direct visualization by placing 1-mm-thick films of the samples on the object, as shown in Figure 10. As evident [Fig. 10(c)], no significant color was developed in the PC/PMMA-$Na^+$MMT nanocomposites with 0.287 phr clay. This might be due to the absence of any organic modifier in the unmodified clays, which led to color formation during high temperature melt-processing of PC/clay nanocomposites. The (80/20 w/w) PC/PMMA-$Na^+$MMT nanocomposites with 0.287 phr clay showed excellent transparency, indicating retention of good optical property of PC in the nanocomposites. We assumed that the high optical clarity of the nanocomposites resulted from the homogeneous dispersion and distribution of the unmodified clay silicates in the PC/PMMA miscible blend.

## CONCLUSION

Well exfoliated PC/$Na^+$MMT nanocomposites without significant loss in optical clarity has been

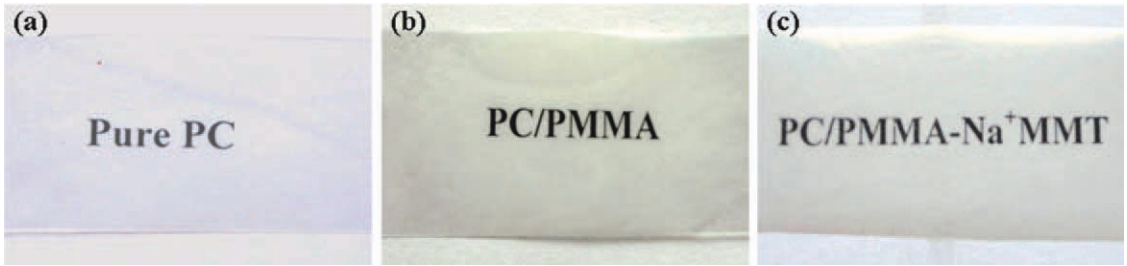


**Figure 10** Optical transparency of (a) pure PC; (b) (80/20 w/w) PC/PMMA blend; and (c) (80/20 w/w) PC/PMMA-$Na^+$MMT nanocomposites with 0.287 phr clay. [Color figure can be viewed in the online issue, which is available at wileyonlinelibrary.com.]

prepared by blending PC with *in situ* suspension polymerized exfoliated PMMA-$Na^+$MMT nanocomposites. The surface morphology study (SEM) and DSC revealed complete miscibility of PC and PMMA in the (80/20 w/w) PC/PMMA blend and PC/PMMA-$Na^+$MMT nanocomposites with 0.287 phr clay. WAXD study and TEM analysis of the (80/20 w/w) PC/PMMA-$Na^+$MMT nanocomposites clearly indicated the exfoliation of the $Na^+$MMT clay in the PC/PMMA-$Na^+$MMT nanocomposites. The thermal stability ($T_{50}$) of the PC/PMMA-$Na^+$MMT nanocomposites was significantly increased compared to the virgin PC. The DMA revealed higher storage modulus of the (80/20 w/w) PC/PMMA-$Na^+$MMT nanocomposites than that of the pure polymers and PC/PMMA blend. The PC/$Na^+$MMT nanocomposites prepared by this method indicated retention of optical transparency of PC in the nanocomposites without any color formation.

Financial support from the DST India is highly acknowledged.

## References


1. Usuki, A.; Hasegawa, N.; Kato, M. Adv Polym Sci 2005, 179, 135.
2. Sinha Ray, S.; Kato, M. Prog Polym Sci 2003, 28, 1539.
3. Li, X.; Kang, T.; Cho, W. J.; Lee, J. K.; Ha, C. S. Macromol Rapid Commun 2001, 22, 1306.
4. Uhl, F. M.; Wilkie, C. A. Polym Degrad Stab 2002, 76, 111.
5. Vyazovkin, D. S. I.; Fan, X.; Advincula, R. J Phys Chem B 2004, 108, 11672.
6. LeGrand, D. G.; Bendler, J. T. Handbook of Polycarbonate Science and Technology; Marcel Dekker: New York, 2000.
7. González, I.; Eguiazábal, J. I.; Nazábal, J. Polym Eng Sci 2006, 46, 864.
8. Carrion, J. F.; Arribas, A.; Bermúdez, M. D.; Guillamon, A. Eur Polym J 2008, 44, 968.
9. Yoon, P. J.; Hunter, D. L.; Paul, D. R. Polymer 2003, 44, 5323.
10. Yoon, P. J.; Hunter, D. L.; Paul, D. R. Polymer 2003, 44, 5341.
11. Mitsunaga, M.; Ito, Y.; Sinha Ray, S.; Okamoto, M.; Hironaka, K. Macromol Mater Eng 2003, 288, 543.
12. Lee, K. M.; Han, C. D. Polymer 2003, 44, 4573.
13. Smith, W. A.; Barlow, J. W.; Paul, D. R. J Appl Polym Sci 1981, 26, 4233.
14. Yoo, Y.; Choi, K. Y.; Lee, J. H. Macromol Chem Phys 2004, 205, 1863.
15. Rama, M. S.; Swaminathan, S. Ind Eng Chem Res 2010, 49, 2217.
16. Huang, X.; Lewis, S.; Brittain, W. J.; Viva, R. A. Macromolecules 2000, 33, 2000.
17. Nevalainen, K.; Vuorinen, J.; Villman, V.; Suikonen, R.; Jarvela, P.; Sundelin, J.; Lepisto, T. Polym Eng Sci 2009, 49, 631.
18. Carroccio, S.; Paglisi, C.; Montaudo, G. Macromolecules 2002, 35, 4297.
19. Puglisi, C.; Sturiale, L.; Motaudo, G. Macromolecules 1999, 32, 2194.
20. Abbas, K. B. Polymer 1981, 22, 836.
21. Abbas, K. B. Polymer 1980, 21, 936.
22. Xie, W.; Geo, Z.; Pan, W.; Hunter, D.; Singh, A.; Vaia, R. A. Chem Mater 2001, 13, 2979.
23. Sinha Ray, S.; Bousmina, M. Macromol Rapid Commun 2005, 26, 450.
24. Sinha Ray, S.; Bousmina, M. Macromol Rapid Commun 2005, 26, 1639.
25. Lim, D. S.; Kyu T. J Chem Phys 1990, 92, 3944.
26. Lim, D. S.; Kue, T. Polym Prepr Am Chem Soc Div Polym Chem 1988, 29–2, 354.
27. Agari, Y.; Ueda, A.; Omura, Y.; Nagai, S. Polymer 1997, 38, 801.
28. Garlund, Z. G. ACS Polym Prepr 1982, 23, 258.
29. Nishimoto, M.; Keskkula, H.; Paul, D. R. Polymer 1991, 32, 272.
30. Kim, C. K.; Paul, D. R. Polymer 1992, 33, 4929.
31. Callaghan, T. A.; Paul, D. R. J Polym Sci Part B: Polym Phys 1994, 32, 1813.
32. Wagner, H. L. J Phys Chem Ref Data 1987, 16, 165.
33. Lee, D. C.; Jang, L. W. J Appl Polym Sci 1996, 61, 1117.
34. Butzbach, G. D.; Wendroff, J. H. Polymer 1991, 32, 1155.
35. Chiou, J. S.; Barlow, J. W.; Paul, D. R. J Polym Sci Part B: Polym Phys 1987, 25, 1459.
36. Saldanha, J. M.; Kyu, T. Macromolecules 1987, 20, 2840.
37. Kue, T.; Saldanha, J. M. Macromolecules 1988, 21, 1021.
38. Sakellariou, P.; Eastmond, G. C. Polymer 1993, 34, 1528.
39. Varughesh, K. T.; Nando, G. B.; De, P. P.; De, S. K. J Mater Sci 1988, 23, 3894.
40. Thomas, S.; George, A. Eur Polym J 1992, 28, 1451.
41. Walsh, D. J.; Higgins, J. S.; Zhikuan, C. Polymer 1982, 23, 336.
42. Thomas, S.; Gupta, B. R.; De, S. K. J Vinyl Technol 1987, 9, 71.
43. Alexander, M.; Dubois, P. Prog Polym Sci 2000, 28, 1.
44. Sinha Ray, S.; Bousmina, M. Prog Mater Sci 2005, 50, 962.
45. Fang, F. F.; Choi, H. J.; Joo, H. J. J Nanosci Nanotechnol 2008, 8, 1559.
46. Bandyoapdhyay, J.; Sinha Ray, S.; Bousmina, M. Macromol Chem Phys 2009, 210, 167.
47. Sikdar, D.; Katti, K. S.; Katti, D. R. J Nanosci Nanotechnol 2008, 8, 1638.
48. Bandyoapdhyay, J.; Sinha Ray, S.; Bousmina, M. Macromol Chem Phys 2007, 208, 1979.